A Pilot Study on Fetal Heart Rate Extraction from Wearable Abdominal Inertial Sensors

Chenxi Yang, *Student Member of IEEE*, Clarel Antoine, M.D., Bruce K. Young, M.D., and Negar Tavassolian, *Senior Member of IEEE*

***Abstract*—This work proposes a novel approach for detecting fetal heart rate (FHR) using seismo-cardiogram (SCG) and gyro-cardiogram (GCG) recordings collected from abdominal inertial sensors. A proof-of-concept setup with commercially available sensor nodes is prepared. The FHR components are extracted from the fused cepstrum of recordings of all the sensors. The feasibility of the proposed method is evaluated with experiments on ten pregnant women under supine, seated, and standing positions. The results are compared with simultaneously-collected recordings of fetal cardiotocography (fCTG). The best position for collecting the signals is deemed to be the supine position, which reports best average root mean square error (RMSE) of 9.83 BPM and average positive percent agreement (PPA) of 84.44% for the SCG signal. The overall results of RMSE are 11.40 BPM from SCG and 12.08 BPM from GCG. The overall reliability from SCG is 75.02%, which is slightly lower than the value of 75.52% from GCG. In summary, the results are comparable between the two modalities, suggesting no significant difference between the usage of the two methods. Our results indicate that wearable inertial sensors could potentially be used to extract FHR outside the clinic with accuracy and reliability metrics comparable to other modalities such as fCTG.**

***Index Terms*—Fetal Heart Rate, Gyro-cardiogram, Seismo-cardiogram, Wearable Sensors.**

I. Introduction

Recent reports indicate that objective and continuous monitoring of fetal heart rate (FHR) and fetal movement could identify fetal compromise with high reliabilities and decrease stillbirth through time-sensitive management [1]. In the United States alone, an average of 26,000 cases of perinatal mortality occur per year, and this rate has barely changed over the past 15 years [2], [3]. In the UK, 29% of stillbirths occur in the absence of complicating factors [4]. This results in an urgent desire for a continuous fetal monitoring (CFM) system that can keep track of both the fetal heart rate and fetal movement [5], [6].

Fetal heart rate (FHR) and fetal movement are the only viable biologic signs that can be continuously monitored and assessed. The fetal heart rate variation (HRV) decreases dramatically days before stillbirth until a loss of HR and HRV occurs several hours before the actual stillbirth [7], [8]. Baseline and acceleration abnormalities have also been reported in the cases of fetal cardiovascular and neural system diseases [9], [10].

A wearable system that could provide continuous and simultaneous monitoring of fetal heart rate and fetal movement outside the clinic could identify the onset of compromise and allow intervention before the occurrence of fetal death. Such monitoring would be valuable not only in women with high risks of stillbirth but also in low-risk pregnancies to prevent stillbirths occurring without apparent complicating factors [11].

Fetal Cardiotocography (fCTG) and fetal electrocardiography (fECG) are two wearable technologies which are widely employed in current clinical settings for monitoring FHR and fetal movements. The fCTG uses external Doppler ultrasound sensors to monitor the FHR and the activity of the uterine muscle [12], [13]. Despite their extensive use, current ultrasound sensors have drawbacks. They may be harmful to the fetus if used over extended periods of time due to teratogenic or fetotoxic effects from ultrasonic heating of fetal tissues [13]. This drawback limits their potential to be used as wearable and continuous home-based monitors. FDA has recommended that current commercial Doppler ultrasound fetal monitors be avoided outside the clinic due to low accuracies as well as unpredictable risks due to unguided usage [14].

The fECG technology uses multiple electrodes to detect FHR and monitors the rotation of the fetus to estimate fetal movement [15], [16]. However, the signal quality of abdominal fECG highly depends on the position of the electrodes with respect to the fetus, and therefore the accuracy is highly variable [17]. There are wireless and wearable sensor patches available which utilize fECG during labor such as AN24 [18] and Avalon (with the wireless transducer) [19]. They are not the most convenient solutions for home-based monitoring due to the need for professional knowledge and skills to prepare and apply the device. Current devices also have notable side-effects such as skin irritation [20].

A series of emerging technologies which are under development can also be used to detect FHR in a wearable setup. Particularly, Fetal Photoplethysmography (fPPG) [21], [22], and Fetal Phonocardiography (fPCG) sense FHR by detecting optical and acoustic signals respectively [23], [24]. These two technologies can detect FHR with lower accuracies and reliabilities compared to fECG [22], [23]. They also lack the capability of monitoring fetal movements [6].

*Research supported by National Science Foundation (NSF) under award number 1855394.

Chenxi Yang is a Ph.D. candidate at the Department of Electrical and Computer Engineering at Stevens Institute of Technology, Hoboken, NJ, 07030 USA.

Clarel Antoine is an Associate Professor at Department of Obstetrics and Gynecology at New York University, New York, NY, 10016.

Bruce K. Young is a Silverman Professor of Obstetrics and Gynecology at Department of Obstetrics and Gynecology at New York University, New York, NY, 10016.

Negar Tavassolian is an Associate Professor at the Department of Electrical and Computer Engineering at Stevens Institute of Technology, Hoboken, NJ 07030 USA. (e-mail: negat.tavassolian@stevens.edu).

There are two main challenges in implementing current technologies as a home-based monitor. The first challenge is that simultaneous monitoring of fetal heart rate and fetal movement using state-of-the-art technology would result in a significant increase in size, complexity, and power consumption of the system. For example, the latest Avalon CL wireless fetal monitor has a large profile of 5.1 kg and a limited battery life of 4 hours [13]. The second challenge is that current technologies require professional knowledge or experience to be properly applied to the subjects.

Inertial sensors were first introduced in the area of fetal movement monitoring in 1986 [25]. Limited research was conducted at the time due to the shortcomings in the resolutions of the sensors and signal processing techniques [26]. With the progress of the micro-electromechanical system (MEMS) technology, interest in using MEMS accelerometers as a tool to investigate fetal well-being increased [27]. For instance, a system was developed which implements an array of three-axis MEMS accelerometers on the pregnant abdomen to monitor fetal movement after 34 weeks of gestation [28]. Results showed that it is feasible to record and analyze fetal activity with the proper placement of the accelerometers on the maternal abdomen [28]-[30].

On the other hand, MEMS accelerometers are widely discussed in the literature for the assessment of adult cardiovascular health outside clinical settings. The sternal seismo-cardiogram (SCG) signal is defined as the recording of the heartbeat-induced micro-vibrations of the chest wall, which can be collected using an accelerometer positioned on the sternum [31]. This signal reflects the mechanical activities of the heart, including the opening and closure of mitral and aortic valves and the maximal blood flow acceleration [32]. Recently, it has been shown that in addition to the linear components, the rotational components of heart-induced chest vibrations also provide insights into heart activities [32], [33]. The term gyro-cardiography (GCG) has been used to refer to the recording of these vibrations, generally by placing a high-resolution MEMS gyroscope on the chest wall of subjects. The aortic valve opening and closure events can be extracted from the fiducial points of SCG and GCG [31], [32], which reveals the potential of these modalities to provide valuable insights into cardiovascular health.

However, no research has been performed to demonstrate the feasibility of using accelerometers or gyroscopes for monitoring fetal heart rate. In this paper, we hypothesize that fetal heart rate could be monitored using proper attachment and processing of seismo- and gyro-cardiogram signals, leading to major improvements in continuous and wearable fetal monitoring outside the clinic. As a pilot study, we evaluate the feasibility of FHR extraction by placing commercially available inertial sensors on the abdominal wall of the subjects. We then apply ensembled cepstrum analysis to the SCG and GCG recordings to extract FHR information. The results are compared with an fCTG monitor which concurrently records FHR during experiments. To the best of our knowledge, this is the first time that the feasibility of FHR extraction is evaluated using abdominal inertial sensors.

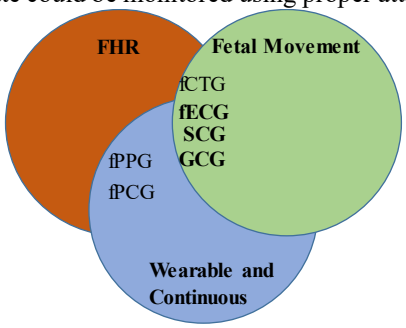

Fig. 1. Venn graph comparing potential technologies.

Fig. 1 illustrates a 3-circle Venn graph to compare the capabilities of the proposed system with competing technologies. Only SCG/GCG, fECG, and fCTG can measure both fetal heart rate and fetal movement. SCG/GCG and fECG have a better long-term and continuous measurement capability compared to fCTG due to the risk concerns of prolonged exposure to ultrasound. Between SCG/GCG and fECG, inertial sensors have a more comfortable setup and do not need any electrode attachments for monitoring. Also, no professional knowledge is needed for the proper implementation of the device. If SCG and GCG can provide reliable fetal HR and movement monitoring, they will be the most suitable technologies for implementation in a home-based wearable monitor.

The layout of this paper is as follows. Section II presents the experimental setup and protocol. The methodology of extracting FHR is introduced in Section III. Section IV summarizes the experimental results and Section V provides discussions of the results. We then conclude the paper and outline the future work in Section VI.

II. Experimental Setup and Protocol

A. Experimental Setup

Fig. 2 illustrates the experimental setup. The reference fCTG is recorded by a FETALGARD Lite system (Version 1.02, using US1 channel), which is shown in Fig. 2 (a). Three commercial wearable sensor nodes (Shimmer 3 from Shimmer Sensing [34]) are attached to the abdominal wall with elastic straps. One sensor node is placed at the center of the upper abdominal wall (Sensor (1) in Fig. 2 (b)). This sensor is close to the reference fCTG ultrasound probe. The remaining two sensors (Sensors (2) and (3) in Fig. 2 (b)) are attached on the lower part of the abdominal wall at symmetric locations. All three sensors are equipped with inertial measurement units (IMU), i.e., accelerometers and gyroscopes. The accelerometers (Kionix KXRB5-2042, Kionix, Inc.) record the seismo-cardiogram (SCG) signal, and the gyroscopes (Invensense MPU9150, Invensense, Inc.) measure the gyro-cardiogram signal (GCG).

The accelerometer and gyroscope ranges are ±2 g and ±250 degrees per second (DPS) respectively, and all the sensor recordings are sampled at a sampling rate of 512 Hz. Data are stored in a memory card on the sensor node and then transmitted to a computer for digital signal processing. The reference CTG and the sensor recordings are synchronized by cross-checking

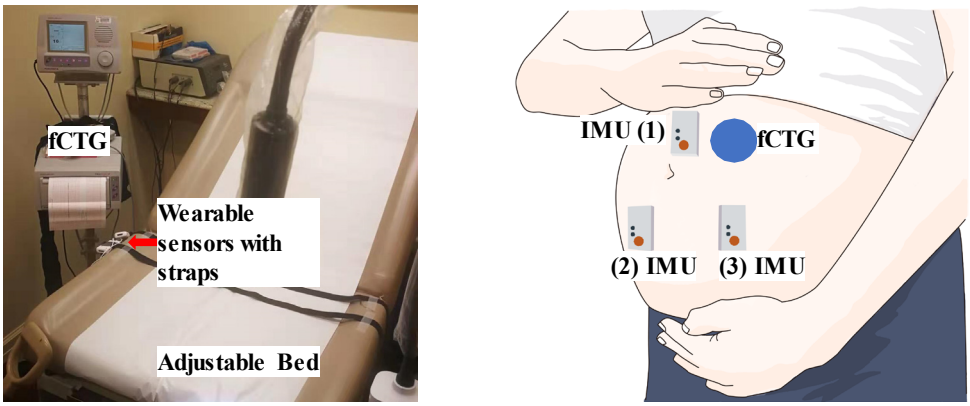

(a) (b)

Fig. 2. (a) Experimental setup and environment. (b) Illustration showing the proof-of-concept setup with three sensor nodes (straps/tapes are not shown).

their timestamps. All the data are then imported into MATLAB® (R2018) for further processing.

B. Experimental Protocol

The experiment is conducted in an fCTG examination room with an adjustable bed as shown in Fig. 2 (a). The experiment consists of three steps. During the first step, the subjects are required to stay in a supine position for five minutes. The subjects then change to a seated position, and the monitoring continues for another five minutes. Afterwards, the subjects stand up and are monitored for an additional five minutes. Subjects breathed naturally without controlling their breathing depths.

Ten pregnant women from the Department of Obstetrics and Gynecology at New York University (NYU) Medical Center participated in this study. The subject group was designed in collaboration with Dr. Bruce Young and Dr. Clarel Antoine, OB/GYNs at NYU Medical Center. The demographic information is summarized in Table I. The patient experimental protocol was approved by the Institutional Review Board of NYU under study number i18-00564. Dr. Antoine evaluated the eligibility of the patients and supervised the experiments in the examination room. Subject 5 only completed the first two steps. Subject 6 completed three steps for three minutes per step. All other subjects finished the experiment with five minutes per step.

III. Signal Processing Method

A. Pre-filtering

In the axis system of the inertial sensors, the *z*-axis refers to the dorso-ventral direction of the body. The *z*-axis of the seismo-cardiogram (SCG) is the most commonly used heart-induced vibration component in the literature [31], [32]. Therefore, we first evaluate the *z*-axis SCG as a pilot study before fusing the information from multiple axes. For the gyro-cardiogram (GCG) modality, the *y*-axis rotation signal is selected due to the higher quality for this axis as reported in [32] and [33].

TABLE I SUMMARY OF DEMOGRAPHIC INFORMATION OF SUBJECTS PARTICIPATED IN EXPERIMENTS.

	Age (years)	Weight (kg)	Height (m)	BMI (during pregnancy)	Gestational Age (Weeks)
Mean	31.5	86.77	1.646	32.09	40.69
Standard Deviation	5.15	12.55	0.04	4.91	0.39

The SCG and GCG recordings from the corresponding axes are first band-pass filtered to focus on the desired frequency components. A zero-phase infinite impulse response (IIR) filter that passes from 0.8 Hz to 50 Hz is used to prefilter the SCG waveforms. Fig. 3 shows a representative filtered SCG signal. The amplitude of the signal is quite small, suggesting a weak vibration from the abdominal surface. The observation from GCG is similar to that from SCG. Therefore, we fuse the information from all three sensors to enhance the signal quality of SCG and GCG separately. The *z*-axis SCG from three sensors are fused, and the *y*-axis GCG from the three sensors are fused, as described in the following section.

B. Signal Fusion of Multiple Sensors

The ensemble of the recordings in time domain is not suitable for analysis since the axes of the signals from different sensors are misaligned due to the abdominal wall being a curved surface. Therefore, the vibration components from different sensors do not align in the same direction and hence the direct summation of the amplitudes would be misleading. We process the signals using time-frequency analysis based on continuous wavelet transform (CWT). CWT converts the signal into the time-frequency domain, so that the desired frequency components can be fused without losing the time-domain variations [35], [36]. The pre-processed SCG and GCG signals are converted by CWT with a Morse wavelet [37].

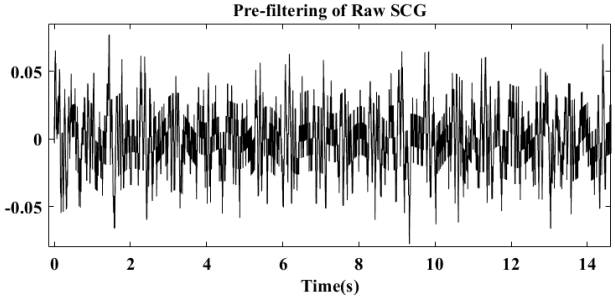

Fig. 3. SCG from the z-axis recording after band-pass filtering.

$$\Psi_{P,\gamma}(\omega) = U(\omega) a_{P,\gamma} \omega^{\frac{P^2}{\gamma}} e^{-\omega^{\gamma}} \quad (1).$$

where P is the time-bandwidth product and γ is the symmetry parameter. In this study, γ is selected as 3 and P is set to 120. The dominant frequency band of the FHR signals is located based on the power distribution of the CWT coefficients. An averaging function then fuses the CWT coefficients from the corresponding frequency band of the three sensors. Then a frequency-selective inverse CWT is conducted to reconstruct a signal that represents FHR. The results from a representative SCG segment are shown in Fig. 4. The top plot in each sub-figure shows the heatmap of the CWT and the bottom plot in each sub-figure illustrates the frequency-selective inverse CWT. The results from each sensor are illustrated in Fig. 4 (a) – (c), followed the results from fused CWT in Fig. 4 (d). It is seen that there are differences among the heatmaps, especially in the dominant band of the vibration signal (1-5 Hz). For instance, the frequency-selective inverse CWT from Sensor (1) shows several attenuated peaks compared to the results from the fused CWT in Fig. 4 (d). A similar observation is also found from the inverse CWT results of Sensor (3) (Fig. 4 (c)). The results from Sensor (2) in Fig. 4 (b) are comparable to the fused results. In summary, signal stability is improved after fusion.

C. FHR Extraction

The spectrums of the fused waveforms are analyzed by the cepstrum method. The cepstrum is defined as the inverse Fourier transform of the real logarithm of the magnitude of the Fourier transform of a time-domain sequence [38]. The method could be presented in the equation below:

$$C_{sig} = real(\mathcal{F}^{-1}\{\log(|\mathcal{F}(x)|)\}). \quad (2)$$

In equation (2), x represents the fused waveform from CWT shown in Fig. 4 (d). The cepstrum is close in definition with the autocorrelation function, which is indexed also by lag time, with the difference that the inverse Fourier transform is taken from the squared spectrum (i.e., power spectral density) instead of the logarithm of the spectrum. The FHR could then be presented as the periodicity in the spectrum, shown as a peak value in the cepstrum located at the corresponding lag time value

Based on the sensor fusion framework introduced above, we then extract FHR from the recordings. The sliding window for

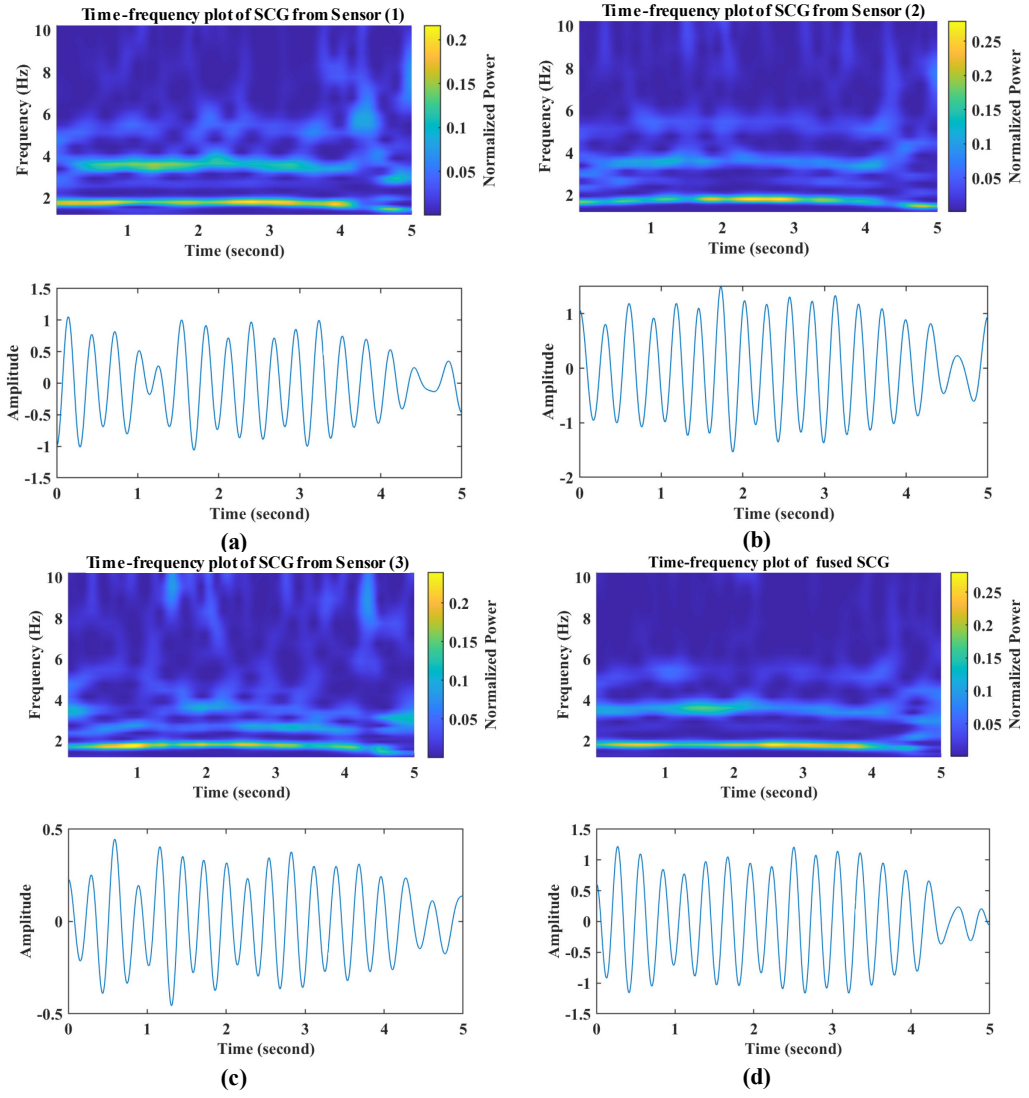

Fig. 4. CWT heatmap and the frequency-selective inverse CWT of SCG from (a) Sensor 1, (b) Sensor 2, (c) Sensor 3, (d) fused CWT. The top plot in each sub-figure shows the heatmap of the CWT and the bottom plot in each sub-figure illustrates the frequency-selective inverse CWT.

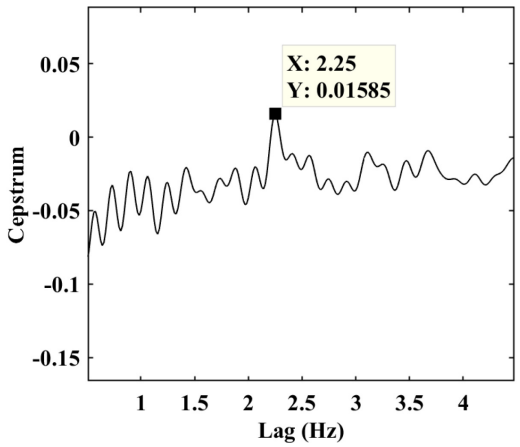

Fig. 5. The cepstrum of the ensembled signals based on SCG. The peak that indicates FHR is labeled and highlighted with a black square.

CWT is set to 5 seconds to approximate the averaging process according to [39]. In this pilot study, the FHR recordings from the reference fCTG range between 120 and 180 BPM. Therefore, we target the FHR within this range. The highest peak that locates in the range from 0.33 to 0.5 seconds (2 Hz to 3 Hz in repeating frequency) is identified as the FHR period.

Fig. 5 shows the cepstrum of a representative section from seismo-cardiogram (SCG) recordings. We can see that there is a detected peak with a lag at 2.25 Hz, highlighted with a black square. As a result, the FHR of this interval is 2.25 × 60 = 135 BPM.

IV. Results

A. Evaluation Metrics

The accuracy and reliability of the proposed signal processing method were evaluated. The accuracy of the FHR detection was analyzed by the Bland-Altman analysis. The errors between fCTG and the proposed method were evaluated using the root mean square error (RMSE) and the absolute percentage error (APE) metrics. These two metrics are based on a time window of 5 seconds. In addition, the average FHR during each step of the experiments was evaluated using the APE metric.

We assessed the reliability of the proposed setup by the positive percent agreement (PPA), i.e., the percentage of time the proposed method generated a valid FHR within 10% of a valid simultaneous FHR from the fCTG [39], [40]. The PPA metric expresses the ability of the proposed method to generate a valid output concurrent with that of the reference device.

B. Fetal Heart Rate Detection

1) FHR Accuracy

We compared the FHR recordings from fCTG to the FHR extraction results from the seismo-cardiogram (SCG) signals and gyro-cardiogram (GCG) signals.

Table II summarizes the results of RMSE and APE from SCG and GCG of all the subjects in supine, seated, and standing positions. It shows that the SCG modality provides an average RMSE of 9.83 BPM with a standard deviation of 1.45 BPM in the supine position. The best and worst results among subjects for each metrics are highlighted in the table with green and red shading respectively. For instance, the best performance among the ten subjects (the smallest RMSE) is from Subject 6 with a value of 8.35 BPM. The worst result among subjects (the largest RMSE) is reported from Subject 2 with a value of 13.09 BPM, suggesting a variation range of 4.74 BPM among subjects. The APE in the supine position gives an average of 6.13% and a standard deviation of 1.23% on average. As highlighted in the table, the best result is 5.14% from Subject 4, and the worst is 8.35% from Subject 2, which reports a range of 3.21% among subjects.

When the subjects change from the supine to the seated position, and from the seated to the standing position, the RMSE and APE metrics based on SCG modality are increased (worsened). For instance, the RMSE is 11.52 BPM on average with a standard deviation of 2.00 BPM, both revealing higher values than the values from the same method in the supine positions (9.83 ±1.45 BPM). The APE metric gives 7.42% ± 1.84% in the seated position in comparison to 6.13% ± 1.23% in the supine position. In the standing position, the RMSE values are further increased to 13.02 ± 1.91 BPM, and the APE metrics step up to 8.29% ± 1.17%.

Compared to the results from SCG in the supine position, the results from GCG suggest slightly higher average RMSE (10.13 BPM vs. 9.83 BPM) and higher standard deviation (2.89 BPM vs. 1.45 BPM). Similarly, GCG shows worse performance in average APE and standard deviation than results from SCG, with a value of 6.39% ± 1.90% compared to 6.13 % ± 1.23% from SCG modality. The ranges of RMSE and APE values from GCG are more extensive than those from SCG, reporting 6.08 BPM (Subject 10) to 14.42 BPM (Subject 4) in RMSE and 4.18% (Subject 10) to 9.65% (Subject 4) in APE. In general, the SCG modality shows slightly better accuracy when subjects are in the supine position.

The results from GCG modality in other positions generally show similar trends to the results from SCG in RMSE metrics and average APE. However, there is a marginal difference in the trend of the standard deviation of APE values. The RMSE results are 12.89 ± 2.04 BPM in the seated position and 13.34 ± 2.88 BPM in the standing position. Furthermore, the APE results report 8.10% on average in the seated position and 7.78 % in the standing position.

The RMSE results in the seated position are slightly higher than results from SCG in the same positions (12.89 ± 2.04 vs. 11.52 ± 2.00 BPM). The standard deviation of RMSE in the standing position is also worse than the value from SCG (2.88 vs. 1.91). The average RMSE from GCG is slightly higher than that from SCG in standing positions, which gives 13.34 BPM in comparison to 13.02 BPM, respectively.

The APE results suggest higher values on average (8.10% vs. 7.42%) but lower values in standard deviation (1.10% vs. 1.84%) than results from SCG in the seated position. In the standing position, the results from GCG are lower on average APE (7.78% vs. 8.29%) but higher in standard deviation (1.73% vs. 1.17%).

In summary, the overall RMSE regardless of the positions from SCG modality reports 11.40 BPM on average with a

TABLE II
ACCURACY RESULTS OF THE FHR EXTRACTION.

Position / Subject	Supine		Seated		Standing		Supine		Seated		Standing	
	RMSE	APE	RMSE	APE	RMSE	APE	RMSE	APE	RMSE	APE	RMSE	APE
Modality	SCG						GCG					
1	8.70	5.14%	8.97	5.81%	10.40	7.30%	12.16	8.53%	13.10	8.07%	16.94	9.24%
2	13.09	8.34%	12.27	7.07%	13.85	9.09%	8.14	4.17%	13.05	8.00%	11.84	6.29%
3	9.30	5.30%	11.66	9.26%	13.73	8.67%	8.30	5.37%	13.10	8.26%	11.49	7.83%
4	9.45	5.50%	12.63	9.89%	15.82	9.80%	14.42	9.65%	14.87	8.32%	13.76	7.07%
5*	9.76	6.36%	13.53	7.53%	N/A	N/A	12.74	6.53%	15.87	9.60%	N/A	N/A
6	8.35	5.67%	12.02	9.74%	13.24	9.74%	8.57	5.31%	12.17	9.39%	11.32	8.11%
7	11.49	8.35%	7.57	4.54%	12.71	7.16%	6.08	4.94%	9.19	6.95%	13.03	7.06%
8	9.17	5.29%	10.40	5.30%	13.14	7.55%	11.59	7.18%	11.15	6.58%	16.86	10.07%
9	8.84	5.30%	12.18	7.71%	9.74	6.60%	12.57	8.01%	15.11	9.19%	8.61	4.65%
10	10.17	6.09%	13.98	7.33%	14.57	8.66%	6.75	4.18%	11.31	6.67%	16.24	9.65%
Mean	9.83	6.13%	11.52	7.42%	13.02	8.29%	10.13	6.39%	12.89	8.10%	13.34	7.78%
Standard Deviation	1.45	1.23%	2.00	1.84%	1.91	1.17%	2.89	1.90%	2.04	1.10%	2.88	1.73%

RMSE: root mean square error (Unit: BPM); APE: absolute percentage error;
Red shading: Largest value among subjects; Green shading: Smallest value among subjects. *Subject 5 only completed first two steps.

standard deviation of 2.17 BPM. In comparison, the results from GCG are higher with 12.08 ± 2.91 BPM. Furthermore, the overall APE from SCG is also lower than the overall APE in both average and standard deviation values, which are 7.25% ±1.66% from SCG and 7.41% ± 1.73% from GCG.

The results summarized in Table II suggest that the overall performances from both modalities are comparable with slightly better results from SCG modality. Regardless of the modalities used, the best position for measurements is the supine position.

2) APE of Average FHR

The APE results of long-term average FHR are shown in Fig. 6. The APE of average FHR is 3.64% in the supine position and rises to 3.61% in the seated position and 6.25% in the standing position using the SCG modality. The error bars indicate that the standard deviation also has a rising trend, with 2.30%, 2.88%, and 3.14% in supine, seated, and standing positions respectively. On the other hand, the results from GCG give 4.37% ± 3.41%, 4.61% ± 2.56%, and 4.77% ± 2.44 on average and standard deviation APEs in the three positions respectively. Results from both modalities reveal a rising trend of APE statistics from supine to standing positions. In supine and sitting positions, the results from SCG are better than those from GCG. However, SCG results are worse in the standing position. The overall APE regardless of positions from SCG is 4.50%, which is lower than the value of 4.58% from GCG.

In conclusion, the results of average FHR are more satisfactory than short-term sliding averaged FHR. All the APEs are lower than the short-term APEs under the corresponding positions. The overall results in the supine position are the best for both SCG and GCG, showing a similar observation to that from Section IV-(2).

3) Reliability of FHR Extraction

Table III summarizes the reliability evaluation of the FHR extraction. The positive percent agreement (PPA) between results from SCG and those from the reference reports 84.44% ± 3.63% in the supine position with a confidence interval (95%) of ± 2.25%, demonstrating the highest reliability among the three positions. Particularly, the PPA results in the seated position (73.22% ± 12.21%) are 11.22% lower on average and 8.58% higher in standard deviation. CI in the seated position is also larger than that in the supine position, with a value of ±7.57% compared to 2.25%. The lowest average PPA comes from results in the standing position, which shows 66.54% with a standard deviation of 10.46% and a confidence interval of 6.83%. The overall PPA including all three positions reports 75.02% ± 11.81% with a CI of 4.30%.

The results from GCG modality also show the highest PPA in the supine position with 79.78% on average, 11.74% in standard deviation, and 7.28% in CI, all of which are less satisfactory than the corresponding values from SCG. In the seated position, the PPA from GCG shows slightly worse average PPA (71.22% vs. 73.22%), but better standard

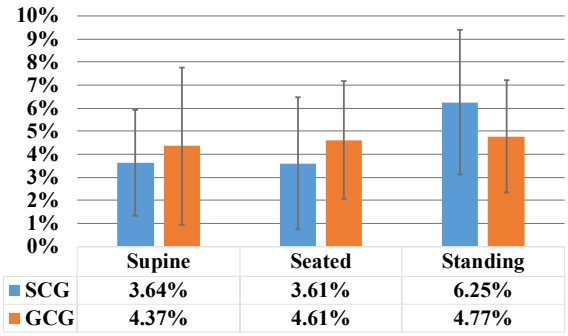

Fig. 6. APE of average FHR. The error bars represent standard deviations.

TABLE III
RELIABILITY RESULTS OF THE FHR EXTRACTION.

Metrics	SCG			GCG		
	Supine	Seated	Standing	Supine	Seated	Standing
PPA	84.44% ± 3.63%	73.22% ± 12.21%	66.54% ± 10.46%	79.78% ± 11.74%	71.22% ± 9.21%	75.56% ± 8.82%
CI	± 2.25%	± 7.57%	± 6.83%	± 7.28%	± 5.71%	± 5.76%
overall PPA	75.02% ± 11.81%			75.52% ± 10.34%		
overall CI	4.30%			3.76%		

deviation (9.21% vs. 12.21%) and CI (5.71% vs. 7.57%) compared to SCG results. Furthermore, the results in standing position show better performance in all three metrics compared to those from SCG, presenting higher average PPA (75.56% vs. 66.54%), smaller standard deviation (8.82% vs. 10.46%), and smaller CI (5.76% vs. 6.83%). The overall PPA of the three positions is 75.52% ± 10.34% with a CI of 3.76%, which are slightly better than the results from SCG. Both modalities show comparable overall reliabilities. The results from SCG are better than those from GCG in the supine position and seated position but worse in the standing position. The position that has the highest reliability is the supine position for both modalities.

V. DISCUSSION

In summary, the position that reports the highest accuracy and reliability is the supine position, with the best RMSE of 9.83 ± 1.45 BPM and PPA of 84.44% ± 3.63%, both from the SCG modality. The overall accuracy and reliability among three positions are comparable between the two modalities, with slightly better performance from SCG than GCG regarding the accuracy, and marginal better reliability from GCG than from SCG.

The comparison of FHR accuracy and reliability between our work and other studies is presented in Table IV. The representative results from this work are shown in the supine position and overall conditions and from the SCG signal. Since there is no study related to FHR extraction with abdominal inertial sensors, we compare the results with abdominal fECG and fCTG methods. As shown in Table IV, the RMSE from fCTG methods in [39] is higher than the results from methods in this work in both average (14.3 vs. 9.83) and standard deviation (8.2 vs. 1.45) values. The results from fCTG in [40] show a slightly higher average RMSE (10.9 vs. 9.83) and a higher standard deviation (5.8 vs. 1.45). However, the RMSE results from fECG methods are much lower than those from our work, demonstrating a better overall performance.

On the other hand, the average PPA from this work is slightly higher than the fECG result from [40] (84.44% vs. 81.7%), and the fECG result from [39] (84.44% vs. 83.4%). Furthermore, this result is higher than results based on fCTG from both works, reporting 62.4% from [39] and 73.0 from [40]. The PPA comparison results suggest that the metrics from this work are comparable with those from fECG, which are higher than the values from fCTG methods.

It is worth mentioning that there are two major differences between our studies and the experiments in [39] [40]. The first difference is that the reference modality used in these two studies is the fetal scalp electrode. In this study, we use an fCTG monitor as the reference. Secondly, the experimental protocols are different. In [39] and [40], the measurements were collected during labor and delivery. In this study, measurements were collected a few days prior to labor and delivery. Although the comparison is not strictly under the same conditions, it suggests the potential of the proposed method to provide FHR monitoring with comparable accuracy and reliability to fCTG and even abdominal fECG.

VI. CONCLUSIONS AND FUTURE WORK

This work proposes a novel approach to detect fetal heart rate (FHR) using seismo-cardiogram (SCG) and gyro-cardiogram (GCG) recordings collected from abdominal inertial sensors. The FHR components are extracted from the ensemble cepstrum analysis results. The feasibility of the proposed method is evaluated with experiments at three different measurement positions. The best position based on the experimental results is the supine position, which reports the best average RMSE of 10.07 BPM and average PPA of 82.89% from SCG methods. The differences of performance between positions might be caused by the differences in attachments of sensors in different positions. The attachments in seated and standing positions are less firm compared to the supine position, reducing the coupling force on the sensor nodes. Maternal movements in seated and standing positions might also be contributing to the degraded performance in these positions. The overall results are comparable between the SCG and GCG modalities, suggesting no significant difference between the feasibility of the two methods. Our results suggest that the proposed solution could be used to track FHR. The accuracy and reliability metrics are less satisfactory than those from fECG but reveal promising potential to be comparable to fCTG devices.

An important challenge for the proposed system is the removal of motion artifacts induced by maternal and fetal movements. In this pilot study, the tests were conducted at rest. In the future, we will evaluate ambulatory scenarios and investigate the use of algorithms that enhance the desired signals and remove other artifacts based on the patterns of the desired signals.

The attachments of the sensors could also be improved by

TABLE IV
PERFORMANCE COMPARISON WITH OTHER RESEARCH METHODS.

Methods	RMSE (BPM)	PPA (%)	CI of PPA	Reference
fCTG1	14.3 ± 8.2	62.4 ± 26.5	N/A	[37]
fCTG2	10.9 ± 5.8	73.0 ± 24.6	5.5	[38]
fECG1	4.8 ± 2.0	83.4 ± 15.4	N/A	[37]
fECG 2	5.3 ± 2.4	81.7 ± 20.5	4.7	[38]
Proposed Method (Supine)	9.83 ± 1.45	84.44% ± 3.63%	2.25	N/A
Proposed Method (Overall)	11.40 ± 2.17	75.20 ± 11.81	4.30	N/A

PPA: Positive Percent Agreement, presented in mean ± standard deviations; CI: Confidence Interval (95%) RMSE: Root Mean Square Error.

using customized stretchable straps with embedded sensors inside. This could ensure firm contact between the abdominal wall and the sensors, improving the mechanical coupling between the skin and the sensor under all positions. A better reference such as fECG could also be used to further validate the performance metrics.

It is to be noted that the subjects in this study have gestational ages of 40.69 weeks on average. The robustness of the proposed system for subjects at earlier gestational weeks is not evaluated. In the future, a larger group of subjects with a more extensive variety of demographic and gestational conditions will be collected. The FHR range studied in this work is from 120 BPM to 180 BPM. Normal FHR range is considered to be from 110 BPM to 160 BPM [8]. The capability of FHR detection with a larger BPM range needs to be further validated to ensure the detection of abnormal conditions such as fetal compromise and heart failure [41]. Furthermore, additional sensors that collect maternal signals non-invasively will be integrated into the system, so that an adaptive algorithm could improve the signal quality, enhancing the accuracy and reliability of FHR monitoring. It is also worth mentioning that the maternal heart signal does not have a significant influence on the recordings of the abdominal inertial sensors. This could be an advantage to abdominal fECG, which requires complicated algorithms to remove maternal ECG components [7]. With further development, the proposed method could show promising potential for the continuous examination of fetus wellbeing and prevention of stillbirth.

REFERENCES

[1] M. F. MacDorman, *et al*, "Fetal and Perinatal Mortality, United States, 2006," *National vital statistics reports: from the Centers for Disease Control and Prevention*, National Center for Health Statistics, National Vital Statistics System, vol. 60, pp.1-22, 2012.

[2] F. J. Korteweg, *et al*. "A Placental Cause of Intra-Uterine Fetal Death Depends on the Perinatal Mortality Classification System Used," *Placenta,* vol. 29, pp. 71–80, 2008.

[3] V. Flenady, *et al.* "An Evaluation of Classification Systems for Stillbirth," *BMC Women's Health*, 2009.

[4] CMACE, "Perinatal Mortality 2009." *Centre for maternal and child enquiries*, United Kingdom, London, 2011.

[5] R. L. Goldenberg, *et al.*, "Stillbirths: The Vision for 2020", *Lancet*, vol. 377, pp.1798–1805, 2011.

[6] Rebecca Brown, *et al.* "Continuous Objective Recording of Fetal Heart Rate and Fetal Movements Could Reliably Identify Fetal Compromise, Which Could Reduce Stillbirth Rates by Facilitating Timely Management," *Medical hypotheses*, no. 3, pp 410-417, 2014.

[7] R. Sameni, G. D. Clifford, "A Review of Fetal ECG Signal Processing; Issues and Promising Directions," *The open pacing, electrophysiology & therapy journal*, vol. 3, no. 4, 2010.

[8] S. Pildner von Steinburg, *et al.* "What is the "Normal" Fetal Heart Rate?" *Pier J*, vol. 1, 2012.

[9] J. F. Froen, *et al.*, "Restricted Fetal Growth in Sudden Intrauterine Unexplained Death", *ActaObstet. Gynecol. Scand.*, vol. 83, pp.801–807, 2004.

[10] Roger K. Freeman, *et al. Fetal heart rate monitoring.* Lippincott Williams & Wilkins, 2012.

[11] Enas W. Abdulhay, *et al.* "Review Article: Non-Invasive Fetal Heart Rate Monitoring Techniques." *Biomedical Science and Engineering*, vol. 2, no. 3, pp. 53-67, 2014.

[12] B. K. Young, *et al.* "Observations in Perinatal Heart Rate Monitoring. I. A Quantitative Method of Describing Baseline Variability of The Fetal Heart Rate." *The Journal of reproductive medicine*, vol. 20, no. 4, pp.205-212, 1978.

[13] K. Nicolaides, *et al.* "Doppler in obstetrics." 2002. Available from: <http://www.fetalmedicine.com/fmf/ Doppler%20in%20Obstetrics.pdf>.

[14] Avoid Fetal "Keepsake" Images, Heartbeat Monitors. Available at: https://www.fda.gov/ForConsumers /ConsumerUpdates/ucm095508.htm

[15] R. Vullings, *et al.* "Fetal Movement Quantification by Fetal Vectorcardiography: A Preliminary Study,", *Conf. Proc. IEEE Eng. Med. Biol. Soc.*, 2008.

[16] E. M. Graatsma, "Monitoring of fetal heart rate and uterine activity." Doctoral dissertation, Utrecht University, 2010.

[17] E. M. Graatsma, *et al.* "Fetal Electrocardiography: Feasibility of Long-term Fetal Heart Rate Recordings." *BJOG: An International Journal of Obstetrics & Gynaecology*, vol. 116, no. 2, pp. 334-338, 2009.

[18] Monica, Introducing the Monica AN24. Available from http://www. monicahealthcare.com/products/ .

[19] Avalon fetal monitor. Available at: https://www.usa.philips.com/ healthcare/resources/landing/avalon

[20] A. Fanelli, *et al.* "Prototype of A Wearable System for Remote Fetal Monitoring During Pregnancy." *Conf Proc IEEE Eng Med Biol Soc*, pp.5815, 2010.

[21] T. H. Sree, *et al.* "Microcontroller Based Fetal Heart Rate Monitoring using Intelligent Biosystem", *3rd International Conference on Electronics, Biomedical Engineering and its Applications (ICEBEA'2013)*, April 29-30, 2013, Singapore.

[22] K. B. Gan, E. Zahedi, and M. M. Ali, "Investigation of Optical Detection Strategies for Transabdominal Fetal Heart Rate Detection Using Three-Layered Tissue Model and Monte Carlo Simulation." *Optica Application*, vol. 41, no. 4, pp. 885-896, 2011.

[23] Martinek, Radek, *et al.* "A Phonocardiographic-based Fiber-Optic Sensor and Adaptive Filtering System for Noninvasive Continuous Fetal Heart Rate Monitoring." *Sensors*, vol. 17, no. 4, pp. 890, 2017.

[24] Kovács, Ferenc, M. Torok, and István Habermajer. "A Rule-Based Phonocardiographic Method for Long-term Fetal Heart Rate Monitoring," *IEEE Transactions on Biomedical Engineering*, vol. 47, no.1, pp. 124-130, 2000.

[25] D. G. Talbert, *et al.* "Wide Bandwidth Fetal Phonography Using a Sensor Matched to the Compliance of the Mother's Abdominal Wall.", *IEEE Transactions on Biomedical Engineering*, vol. 2, pp. 175-181, 1986.

[26] Vasant Padmanabhan, John L. Semmlow, and Walter Welkowitz. "Accelerometer-type Cardiac Transducer for Detection of Low-Level Heart Sounds." *IEEE Transactions on Biomedical Engineering*, vol. 40, no.1, pp. 21-28, 1993.

[27] Nishihara, Kyoko, *et al.* "A Long-Term Monitoring of Fetal Movement at Home Using A Newly Developed Sensor: An Introduction of Maternal Micro-Arousals Evoked by Fetal Movement During Maternal Sleep." *Early human development*, vol.84, no.9, pp. 595-603, 2008.

[28] Boashash, Boualem, *et al.* "Passive Detection of Accelerometer-Recorded Fetal Movements Using A Time–Frequency Signal Processing Approach." *Digital Signal Processing*, pp. 34-155, 2014.

[29] Altini, Marco, *et al.* "Detection of Fetal Kicks Using Body-Worn Accelerometers During Pregnancy: Trade-Offs Between Sensors Number and Positioning." *In Engineering in Medicine and Biology Society (EMBC), 2016 IEEE 38th Annual International Conference of the*, pp. 5319-5322. IEEE, 2016.

[30] Mesbah, M., *et al.* "Accelerometer-based Fetal Movement Detection." *Engineering in Medicine and Biology Society, EMBC, 2011 Annual International Conference of the IEEE.*
[31] M. Etemadi and O. T. Inan, "Wearable Ballistocardiogram and Seismocardiogram Systems for Health and Performance," *Journal of Applied Physiology*, v. 124, no. 2, pp. 452-461, 2018.
[32] C. Yang, N. Tavassolian, "Combined Seismo- and Gyro-cardiography: A More Comprehensive Evaluation of Heart-Induced Chest Vibrations," *IEEE Journal of Biomedical and Health Informatics*, vol. 22, no. 5, pp. 1466-1475, September 2018.
[33] M. J. Tadi, *et al.*, "Gyrocardiography: A New Non-invasive Monitoring Method for the Assessment of Cardiac Mechanics and the Estimation of Hemodynamic Variables." *Scientific Reports*, vol.7, 2017.
[34] Shimmer Sensing. (2019). [Online]. Available: www. shimmersensing.com
[35] F. Bousefsaf, *et al.,* "Continuous Wavelet Filtering on Webcam Photoplethysmographic Signals to Remotely Assess the Instantaneous Heart Rate." *Biomedical Signal Processing and Control*, vol. 8, no.6, pp.568-574, 2013.
[36] Y. Zhang, *et al.*, "Motion Artifact Reduction for Wrist-Worn Photoplethysmograph Sensors Based on Different Wavelengths" *Sensors*, vol. 19, no. 3, p.673, 2019.
[37] A. Taebi, H. A. Mansy, "Time-Frequency Distribution of Seismocardiographic Signals: A Comparative Study." *Bioengineering*, vol. 4, no. 2, pp. 32, 2017.
[38] C. Brüser, *et al.*, "Improvement of Force-Sensor-Based Heart Rate Estimation Using Multichannel Data Fusion," *IEEE Journal of Biomedical and Health Informatics*, vol. 19, no. 1, pp. 227-235, Jan. 2015.
[39] T.Y. Euliano, *et al.* "Monitoring Fetal Heart Rate During Labor: A Comparison of Three Methods." *Journal of pregnancy*, 2017.
[40] W.R. Cohen, *et al.* "Accuracy and Reliability of Fetal Heart Rate Monitoring Using Maternal Abdominal Surface Electrodes." *Acta obstetricia et gynecologica Scandinavica*, vol. 91, no. 11, pp.1306-1313, 2016.
[41] American Academy of Pediatrics, American College of Obstetricians and Gynecologists Fetal heart rate monitoring, *Guidelines for perinatal care.* 7th ed. Washington, DC: American College of Obstetricians and Gynecologists, 2012.

Chenxi Yang (S'13) received the B. Eng. degree in Measuring Control Technology & Instruments from Southeast University, Nanjing, China, in 2013, and the M. Eng. degree in electrical engineering from Stevens Institute of Technology, Hoboken, NJ, in 2015. He is currently working towards his Ph.D. in electrical engineering at Stevens Institute of Technology. His research interests are biophysical signal processing and mobile healthcare with sensor networks. He is a student member of the IEEE Signal Processing Society, Circuits and Systems Society, and Engineering in Medicine and Biology Society. He has received the Edward Peskin Award for an Outstanding Master's Thesis at Stevens Institute, a conference travel award for his paper at BIOCAS 2015, Atlanta, GA, and the NSF EMBC Award for Young Professionals on Smart and Connected Health at EMBC 2016, Orlando, FL.

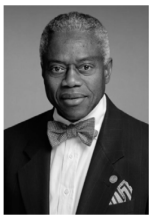

Clarel Antoine, MD is an obstetrician-gynecologist and is affiliated with NYU Langone Hospitals. He received his medical degree from Columbia University College of Physicians & Surgeons and has been in practice for more than 20 years. He completed his residency at Columbia Presbyterian Medical Center, and clinical and research fellowships at Bellevue Hospital Center and NYU Medical Center. He is currently an Associate Professor at the Department of Obstetrics and Gynecology at New York University, School of Medicine.

Bruce K. Young, MD is an obstetrician-gynecologist and is affiliated with NYU Langone Hospitals. He received his medical degree from New York University. He completed his residency at NYU Medical Center and Bellevue Hospital Center, and clinical and research fellowships at NYU Medical Center. He is the founder and the former director of the first maternal-fetal medicine program at NYU Medical Center. He is currently the director of NYU Pregnancy Loss Prevention Center. He is the Silverman Professor of Obstetrics and gynecology at Department of Obstetrics and Gynecology at New York University, School of Medicine. He has lectured worldwide and has earned numerous awards, including the March of Dimes Award for Distinguished Voluntary Service in Prevention of Birth Defects, the Distinguished Alumnus Award from the Department of Obstetrics and gynecology at the NYU School of Medicine, the American College of Obstetricians and Gynecologists Award for Outstanding Achievement, and the Berson Award of the NYU School of Medicine for Achievement in Clinical Science. He has published 122 peer-reviewed articles, more than a dozen invited book reviews and chapters, two medical books, and two books for the general public.

Negar Tavassolian (S'03–M'11–SM'18) is an Associate Professor at the Department of Electrical and Computer Engineering at Stevens Institute of Technology, where she directs the Bio-Electromagnetics Laboratory. She received the B.Sc. and M.Sc. degrees in electrical engineering from Sharif University of Technology, Tehran, Iran, and McGill University, Montreal, Canada, in 2003 and 2006, respectively. She received the Ph.D. degree in electrical engineering from Georgia Institute of Technology in 2011 and was a Postdoctoral Associate at the David H. Koch Institute for Integrative Cancer Research at Massachusetts Institute of Technology from 2011 to 2013. Dr. Tavassolian was an Assistant Professor at Stevens Institute of Technology from 2013 to 2019. She is a recipient of the NSF CAREER award in 2016 and the Provost Early Career Award for Research Excellence in 2018. She a senior member of IEEE since 2018 and a Technical Program Committee member of IEEE MTT-10: Biological Effects and Medical Applications of RF and Microwaves since 2015. Her research is funded by the National Science Foundation and the US Army Medical Research and Material Command.